

Article

Green Synthesis and Electrochemical Properties of Mono- and Dimers Derived from Phenylaminoisoquinolinequinones

Juana Andrea Ibacache ^{1,*}, Jaime A. Valderrama ^{2,*}, Judith Faúndes ¹, Alex Danimann ¹, Francisco J. Recio ³  and César A. Zúñiga ³ 

¹ Facultad de Química y Biología, Universidad de Santiago de Chile, Alameda 3363, casilla 40, Santiago 9170022, Chile; judith.faundes@usach.cl (J.F.); alex.danimann@usach.cl (A.D.)

² Facultad de Ciencias de la Salud, Universidad Arturo Prat, casilla 121, Iquique 1100000, Chile

³ Facultad de Química y Farmacia, Universidad Católica de Chile, casilla 306, Santiago 7820436, Chile; javier.recio@uc.cl (F.J.R.); czuniga1@uc.cl (C.A.Z.)

* Correspondence: juana.ibacache.r@usach.cl (J.A.I.); jaimeadolfov@gmail.com (J.A.V.); Tel.: +562-27181145 (J.A.I.); +569-94781987 (J.A.V.)

Received: 28 October 2019; Accepted: 26 November 2019; Published: 30 November 2019



Abstract: In the search for new quinoid compounds endowed with potential anticancer activity, the synthesis of novel heterodimers containing the cytotoxic 7-phenylaminoisoquinolinequinone and 2-phenylaminonaphthoquinone pharmacophores, connected through methylene and ethylene spacers, is reported. The heterodimers were prepared from their respective isoquinoline and naphthoquinones and 4,4'-diaminodiphenyl alkenes. The access to the target heterodimers and their corresponding monomers was performed both through oxidative amination reactions assisted by ultrasound and $\text{CeCl}_3 \cdot 7\text{H}_2\text{O}$ catalysis “in water”. This eco-friendly procedure was successfully extended to the one-pot synthesis of homodimers derived from the 7-phenylaminoisoquinolinequinone pharmacophore. The electrochemical properties of the monomers and dimers were determined by cyclic and square wave voltammetry. The number of electrons transferred during the oxidation process, associated to the redox potential $E^{1/2}$, was determined by controlled potential coulometry.

Keywords: twin drugs; heterodimers; green synthesis; amination reaction; cyclic voltammetry; half-wave potential

1. Introduction

Quinones are ubiquitous in nature and comprise one of the largest classes of anticancer agents [1–3]. Among the broad variety of drugs used clinically in the therapy of solid cancers, mitomycin, mitoxantrone, and saintopin contain the common quinone nucleus into their active pharmacophores. The most remarkable characteristics of these quinoid drugs are their abilities to act as DNA intercalators, reductive alkylators of biomolecules, and/or generators of reactive oxygen species (ROS) such as hydroxyl radical, hydrogen peroxide, superoxide anion, and singlet oxygen [4], which can damage tumor cells [5–12] via oxidative stress [5,13,14]. It is worth to note that in spite of the broad range of effects of quinoid compounds on grown inhibition of diverse cancer cells, the major limitations, in terms of their use as cancer drugs, are their side effects [15].

A common aminoquinoid unit appeared as a key structural scaffold in diverse natural occurring cytotoxic compounds, such as smenospongine [16,17], streptonigrin [18–23], mansouramicyn C [24,25] and, synthetic cytotoxic 1,4-benzoquinones, 1,4-naphthoquinones [26,27], and heterocyclic analogs [28–32].

A number of synthetic aminoisoquinolinequinones and polycyclic analogs have been the subject of study for many years due to their in vitro cytotoxic activities on several cancer cell lines [33–39].

A well-established procedure to prepare alkyl- and arylaminoquinones is based on the oxidative coupling reaction of quinones with alkyl- and arylamines [40–44]. It is widely accepted that the oxidative coupling reaction involves a Michael addition of the nitrogen nucleophiles to the quinones, followed by oxidation of the hydroquinone intermediates [44].

In Figure 1, representative synthetic phenylaminoquinones endowed with *in vitro* cytotoxic properties against a number of human cancer cell lines are depicted [26,30–32]. The common feature of these aminoquinones to target cancer cells has been attributed, in part, to their abilities to produce oxidative stress via generation of reactive oxygen species (ROS) [45,46].

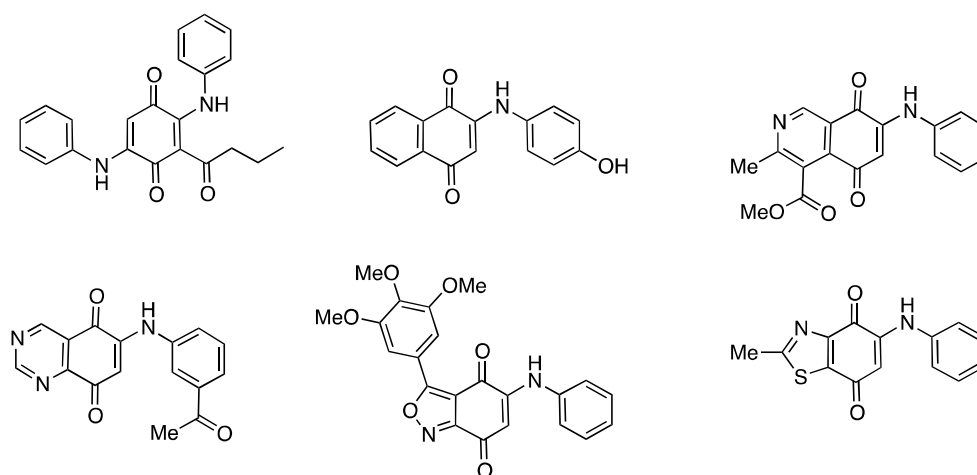
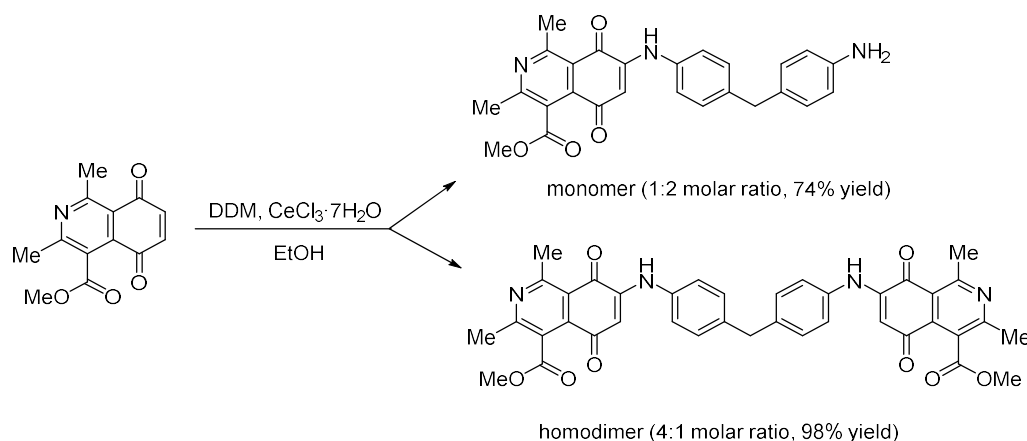


Figure 1. Structure of biological active phenylaminoquinones.

The biological activity of quinones is often related to their electrochemical behavior [47–52]. The ability of the quinone nucleus to accept one or two electrons to give the corresponding semiquinone radical anion ($Q^{\bullet-}$) or hydroquinone dianion (Q^{2-}) species is believed to induce formation of reactive oxygen species (ROS), responsible for the oxidative stress in cells [11,47,53].

Recently, we successfully applied the twin-drug approach [54] to improve the antiproliferative activity and selectivity of the phenylaminoisoquinolinequinone pharmacophore [29,55]. The designed homodimers were prepared through a one-pot procedure from phenylaminoisoquinolinequinones and 4,4'-diaminodiphenylmethane (DDM). It was also reported the selective access to monomers, which are involved in the formation of homodimers [54]. The following Scheme 1 exemplifies the selective access to the corresponding monomer or homodimer employing suitable molar ratio between the quinone and diamine precursors.



Scheme 1. Selective access to a monomer and its homodimer containing the nitrogen pharmacophore.

The selective access to the monomers and the cytotoxic levels of the monomers and homodimers [54] encourage us to extend our studies to the synthesis of heterodimers constituted by anilinoisoquinolinequinone and 2-anilino-naphthoquinone pharmacophores connected through methylene spacers [26]. Bearing in mind that monomers and dimers exhibit one and two electro-active quinone nucleus, respectively, we were also interested to get insight into their electrochemical properties. Herein we report results on the eco-friendly access to monomers, heterodimers, and homodimers derived from isoquinolinequinones, naphthoquinones, and 4,4'-diamino diphenyl alkanes. The new synthesized monomers and dimers were subject to electrochemical studies by cyclic voltammetry, square wave voltammetry, and controlled potential coulometry.

2. Results

2.1. Chemistry

The strategy to construct the heterodimers, where the phenylamino groups of the selected quinoid pharmacophores are connected through methylene spacers, is based on oxidative monoamination reactions of the parent isoquinolinquinones **1** and **2** with the 4,4'-diamino diphenyl alkanes **3** and **4** followed by amination reactions of the resulting monomers with naphthoquinones **8** and **9** (Figure 2).

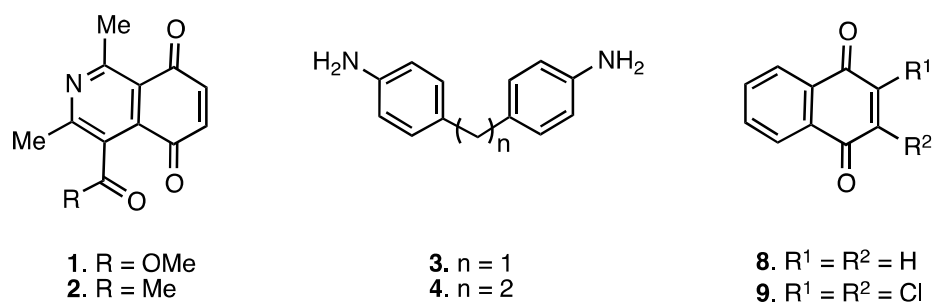
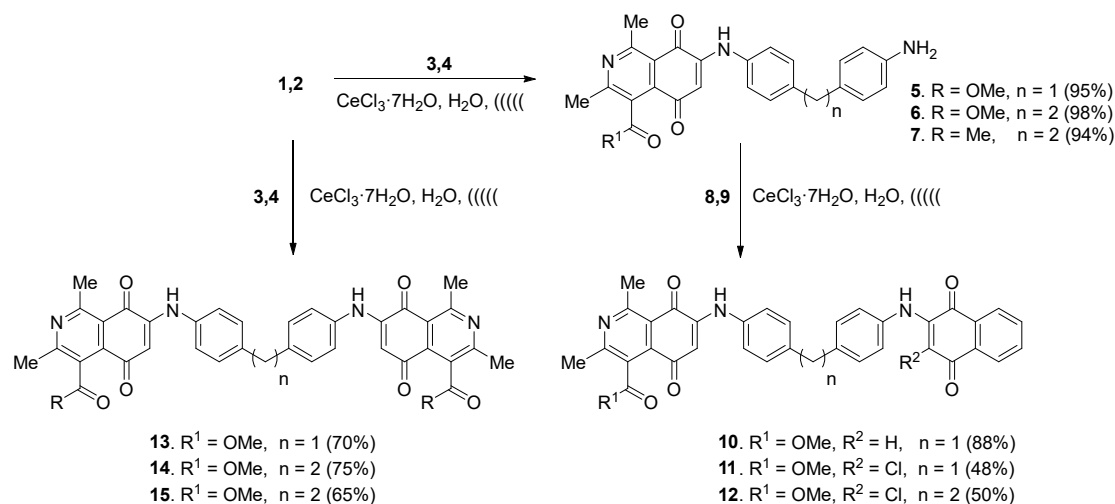


Figure 2. Precursor of phenylaminoisoquinolinquinone-containing monomers and heterodimers.

The access to the designed heterodimers **10**, **11**, and **12** was planned through the aminoisoquinolinequinone monomers **5**, **6**, and **7** resulting from the reaction between the quinones **1/2** and symmetrical diamines **3/4**. The synthetic approach to heterodimer **10** was firstly examined from isoquinolinequinone **1**, naphthoquinone **8**, and diamine **3**. The required monomer precursor **5** was synthesized in 74% yield, according to our previously reported procedure [54], by reaction of the quinone **1** with diamine **3** in a 1:2 mole ratio, catalytic amounts of CeCl₃·7H₂O in ethanol at room temperature [29]. Further reaction assays of **5** with naphthoquinone **9** in a 1:2 ratio under the above-mentioned conditions, performed at room temperature and, in refluxing ethanol, produced heterodimer **10** albeit in low yields (22% and 28%, respectively). The heterodimer **10** was isolated as a purple solid, m.p. 186 °C (d). The IR spectrum reveals the presence of N–H and C=O bands at ν/cm^{-1} : 3337, 1720, 1666, and 1673, respectively. The ¹H-NMR spectrum shows the signals of two vinylic protons at δ 7.54 and 7.67 ppm and the amino proton signals at δ 7.54 and 7.67 ppm. In the aromatic proton region, the proton signals of the naphthoquinone fragment, at δ : 7.67, 7.76 and 8.11, were observed and those of the protons of the phenyl groups of the linker that appeared as a multiplet at δ 7.21 ppm. The methylene protons of the spacer are observed at 4.00 ppm. The ¹³C-NMR spectrum displays signals of three carbonyl groups at δ : 181.5, 181.1, 180.4, and the mass spectrum shows the molecular ion [M⁺] peak at m/z 598.1971.

Interestingly, when a water suspension containing compounds **5** and **9** (1:2 mole ratio) and CeCl₃·7H₂O were ultrasound-irradiated [56] for 6 h, heterodimer **10** was generated and isolated in 88% yield (Scheme 2). Based on this excellent outcome, we decided to extend this green procedure to the synthesis of monomers **5–7** and heterodimers **11** and **12**. The reactions that were conducted under irradiation period of 1.5–7 h, produced the respective monomers **5–7** in excellent yields (94–98%),

and compounds **11** and **12** in moderate yield (48% and 50%) (Scheme 2). The lower yields formation of heterodimers **11** and **12** compared to that of dimer **10** could be attributed to steric hindrance interactions involved in the addition of the nitrogen nucleophiles **11** and **12** across the disubstituted electrophilic quinone double bond of **9**.



Scheme 2. Preparation of hetero- and homodimers from quinones **1**, **2**, **8**, **9** and diamines **3** and **4**.

The one-pot access to homodimers **13–15** from their respective isoquinolinquinones **1** and **2** and their symmetrical diamines **3** and **4** were also carried out under ultrasound irradiation, catalyzed with CeCl₃·7H₂O in water. Under these conditions, the respective homodimers **13–15** were isolated in good yields (65–75%) (Scheme 2).

The structures of the new compounds **6**, **7**, **10–12**, **14**, and **15** were established by infrared spectroscopy (IR), ¹H- and ¹³C-nuclear magnetic resonance (NMR), bidimensional nuclear magnetic resonance (2D-NMR), and high-resolution mass spectroscopy (HRMS).

2.2. Electrochemistry

The monomers **5–7** and dimers **10–12**, **14**, and **15** were evaluated for their half-wave potentials ($E^{I/2}$ and $E^{II/2}$). For all the compounds, the first faradaic process ($E^{I/2}$) presents a reversible behavior, and the second process is quasi-reversible. In Table 1, the electrochemical parameters determined in this study are summarized. The net charge consumption was used to calculate the number of electrons for each compound. In the monomers (**5–7**), the values of charge are close to 10 mC, which indicate a one-electron transfer during the faradaic process. However, for the heterodimers and homodimers it is close to 20 mC under the studied conditions, which implies 2-electrons. These transferred electron values were corroborated by the following equation: $|E_{pc} - (E_{pc}/2)| = \frac{90.6}{n}$ for an ideal reversible peak ($E^{I/2}$), where E_{pc} is the cathodic peak potential and $E_{pc}/2$ is potential at half-width of the cathodic peak for all the studied molecules [57–59].

The first potential for compounds **5–7** (via one-electron), and, for dimers **10**, **11**, **12**, **14–15** (via two-electrons) produce the corresponding semiquinone radical anion(s) [6,13,14]. The first and second reduction potential of monomer **5** correspond to the monoelectronic transfer processes: E^I : $Q + e^- = \text{semiquinone radical anion } (Q^{\bullet-})$ and E^{II} : $Q^{\bullet-} + e^- = \text{quinone dianion } (Q^{2-})$ [60,61]. It is important to note that in the case of dimers **10**, **11**, **12**, **14**, and **15**, a broad faradaic process associated to the overlap between $E^{I/2}$ and $E^{II/2}$ is detected due to the conjugate nature of the benzene ring groups together with the fast-kinetic reaction of the carbonyl groups [62,63].

Figure 3 shows the voltammograms for monomer **5–7** and homo- and heterodimer **10–12**, **14–15** (Supplementary Figures S1–S8, Cyclic voltammetry and square wave voltammetry (SWV)).

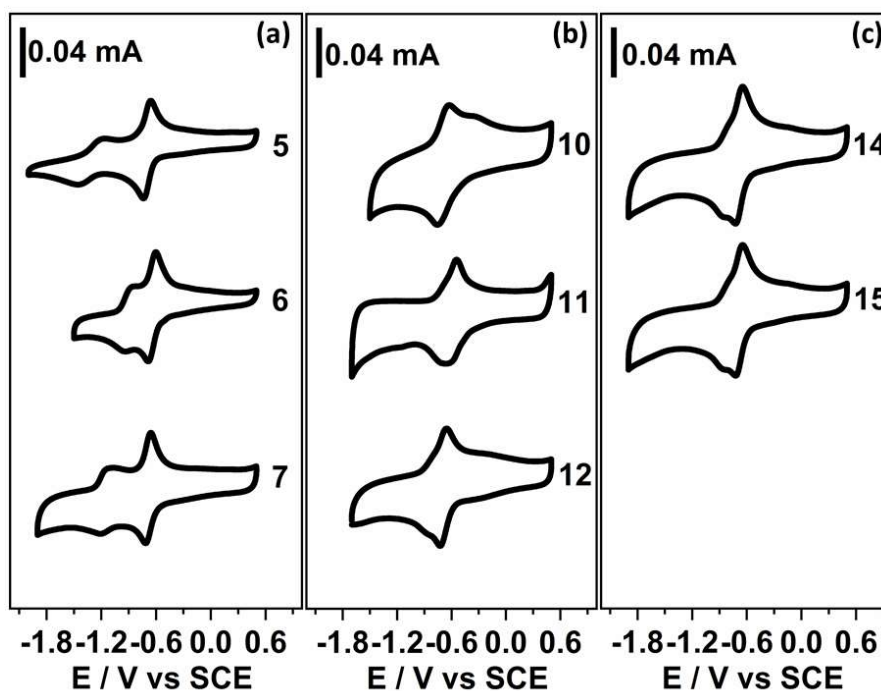
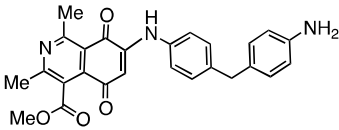
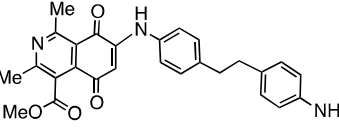
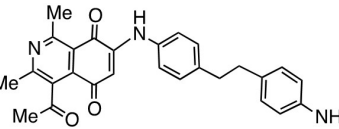
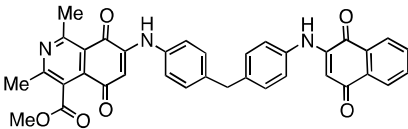
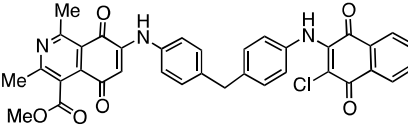
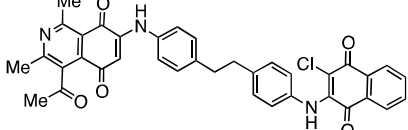
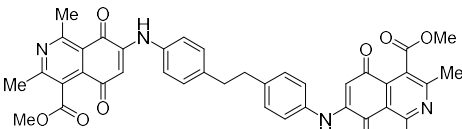
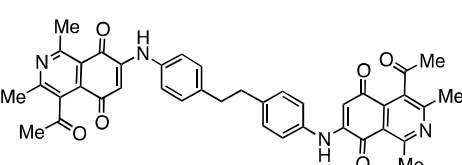


Figure 3. Cyclic voltammetry 100 mV s^{-1} of (a) monomers **5**, **6**, **7**; (b) heterodimers **10**–**12**; (c) homodimers **14**, **15**; with a concentration of 0.1 M of the molecules studied in 0.1 M tetrabutylammonium perchlorate (TBAP) in acetonitrile and saturated N_2 atmosphere.

The electrochemical parameters presented in Table 1 indicate that monomers **5**–**7** exhibited a relative closeness in the values of the potential $E^{I_{1/2}}$ and $E^{II_{1/2}}$ and widening of the faradic signal associated with both processes. These facts could be attributed to the electronic nature of the substituents of the compounds [46]. In the case of heterodimers **10** and its chlorine analog **11**, the shift to more positive values of $E^{I_{1/2}}$ and $E^{II_{1/2}}$ of the later with respect to **10** could be attributed to the electron-withdrawing effect of the chlorine atom. Similarly, the shift to more positive values of $E^{I_{1/2}}$ of monomer **6** compared to **7**, and homodimer **14** compared to **15** could be explained by the stronger electron-withdrawing ability of the methoxycarbonyl group in **14** than the acetyl group in **15**. These results agree with precedents on the influence of electron-withdrawing substituents in aminoquinones groups, on their oxidant properties [64–67].

The data analysis led us also to found differences between the potential $E^{I_{1/2}}$ and $E^{II_{1/2}}$ of dimers and monomers containing the 4,4'-diaminodiphenylalkane fragment in terms of the nature of the alkane spacers. The comparison of the monomers **5** and **6**, which differ in the chain length of the alkane spacers, shows that the formal potentials of the ethylene-containing monomer **6** appeared at more positive values than its methylene-containing analog **5**. Additional examples are required to establish the influence of the chain length on the potential $E^{I_{1/2}}$ and $E^{II_{1/2}}$.

Table 1. Electrochemical parameters of compounds 5–7, 10–12, and 14–15.

Compound N ^o	Structure	$-E^{I/2}$ (mV) ^a	$-E^{II/2}$ (mV) ^a	n ^b
5		697	1318	1.1
6		681	897	1.2
7		688	1174	1.2
10		661	-	2.0
11		580	-	1.7
12		667	-	1.9
14		652	-	1.8
15		689	-	1.9

^a The formal potentials were obtained as $E_{1/2} = (E_{pa}^I + E_{pc}^I)/2$. ^b Number of electrons transferred calculated for the first formal potential ($E^{I/2}$).

3. Materials and Methods

3.1. General

All solvents, reagents, and precursors such as quinones **8** and **9** were purchased from different companies such as Aldrich (St. Louis, MO, USA) and Merck (Darmstadt, Germany) and were used as supplied. Melting points were determined on a Stuart Scientific SMP3 (Bibby Sterilin Ltd., Staffordshire, UK) apparatus and are uncorrected. The IR spectra were recorded on an FT IR Bruker spectrophotometer; (model Vector 22 Bruker, Rheinstetten, Germany), using KBr disks, and the wave numbers are given in cm^{-1} . ^1H - and ^{13}C -NMR spectra were recorded on a Bruker Avance-400

instrument (Bruker, Ettlingen, Germany) in CDCl_3 at 400 and 100 MHz, respectively. Chemical shifts are expressed in ppm downfield relative to tetramethylsilane and the coupling constants (J) are reported in hertz. Data for $^1\text{H-NMR}$ spectra are reported as follows: s = singlet, br s = broad singlet, d = doublet, m = multiplet, and the coupling constants (J) in Hz. Bidimensional NMR techniques were used for signal assignments. HRMS-ESI were carried out on a Thermo Scientific Exactive Plus Orbitrap spectrometer (Thermo Fisher, Bremen, Germany) with a constant nebulizer temperature of 250 °C. The experiments were performed in positive ion mode, with a scan range of m/z 100–300. All fragment ions were assigned by accurate mass measurements at high resolution (resolving power: 140,000 FWHM). The samples were infused directly into the electrospray ionization source (ESI) using a syringe pump at flow rates of $5 \mu\text{L min}^{-1}$. Silica gel Merck 60 (70–230 mesh, from Merck, Darmstadt, Germany) was used for preparative column chromatography and TLC aluminum foil 60F254 for analytical thin-layer chromatography (TLC). Isoquinolinequinones 1–2 were prepared by previously reported procedures [40].

The ultrasound-promoted reactions were carried out in standard oven-dried glassware in a Branson sonicator cup horn working at 19.7–20.0 kHz (75 W).

3.2. Chemistry

3.2.1. Preparation of Monoamination Compounds 5–7. General Procedure

Suspensions of quinones 1–2 (1 mmol) and corresponding diamine (2 equiv), $\text{CeCl}_3 \cdot 7\text{H}_2\text{O}$ (5 mmol %), and water (20 mL) were left with ultrasonic irradiation after completion of the reaction as indicated by TLC. The reaction mixture was partitioned between chloroform and water, the organic extract was washed with water ($2 \times 15 \text{ mL}$), dried over Na_2SO_4 , and evaporated under reduced pressure. The residue was column chromatographed over silica gel (95:5 $\text{CH}_2\text{Cl}_2/\text{EtOAc}$) to yield the corresponding pure monoamination compounds 5–7.

3.2.2. Preparation of Heterodimers 10–12. General Procedure

Suspensions of compounds 5–7 (2 mmol), naphthoquinone 8/9 (1 mmol), $\text{CeCl}_3 \cdot 7\text{H}_2\text{O}$ (5 mmol %), and water (20 mL) were left with stirring under ultrasonic irradiation after completion of the reaction as indicated by TLC. The reaction mixture was partitioned between chloroform and water, the organic extract was washed with water ($2 \times 15 \text{ mL}$), dried over Na_2SO_4 , and evaporated under reduced pressure. The residue was column chromatographed over silica gel (95:5 $\text{CH}_2\text{Cl}_2/\text{EtOAc}$) to yield the corresponding pure heterodimers 10–12.

3.2.3. Preparation of Homodimers 13–15. General Procedure

Suspensions of quinones 1/2 (4 mmol) and corresponding diamine 3/4 (1 equiv), $\text{CeCl}_3 \cdot 7\text{H}_2\text{O}$ (5 mmol %), and water (20 mL) were left with stirring under ultrasonic irradiation after completion of the reaction. The reaction mixture was partitioned between chloroform and water, the organic extract was washed with water ($2 \times 15 \text{ mL}$), dried over Na_2SO_4 , and evaporated under reduced pressure. The residue was column chromatographed over silica gel (95:5 $\text{CH}_2\text{Cl}_2/\text{EtOAc}$) to yield the corresponding pure homodimers 13–15.

Methyl-7-(4-(4-aminobenzyl)phenyl)amino)-1,3-dimethyl-5,8-dioxo-5,8-dihydroisoquinoline-4-carboxylate (5). m.p. 149–150 °C; IR (KBr) ν/cm^{-1} : 3423 (N-H), 3305, and 3251 (NH_2), 1734 (C=O ester), 1668 (C=O quinone). $^1\text{H-NMR}$ (400 MHz, CDCl_3) δ 2.61 (s, 3H, 3-Me), 2.99 (s, 3H, 1-Me), 3.60 (s, 2H, NH_2), 3.88 (s, 2H, CH_2), 4.00 (s, 3H, CO_2Me), 6.30 (s, 1H, 6-H), 6.62 (dd, $J = 8.3 \text{ Hz}$, 12.8 Hz, 2H), 6.96 (t, $J = 6.8 \text{ Hz}$, 2H), 7.14 (d, $J = 8.3 \text{ Hz}$, 2H), 7.22 (d, $J = 8.3 \text{ Hz}$, 2H), 7.68 (s, 1H, N-H). $^{13}\text{C-NMR}$ (100 MHz, CDCl_3) δ 182.1, 181.7, 169.6, 161.6, 161.3, 146.0, 145.1, 142.7, 140.8, 138.3, 130.9, 130.5, 125.5, 123.4, 120.3, 115.8, 115.7, 102.5, 53.4, 40.9, 26.5, 23.3. HRMS $[\text{M} + \text{H}]^+$: calculated for $\text{C}_{26}\text{H}_{23}\text{N}_3\text{O}_4$: 442.1762; found: 442.1761.

Methyl 7-(4-(4-aminophenethyl)phenylamino)-1,3-dimethyl-5,8-dioxo-5,8-dihydroisoquinoline-4-carboxylate (6). m.p. 212–213 °C; IR (KBr) ν/cm^{-1} : 3465 (NH), 3368, and 3312 (NH₂) 1723 (C=O ester), 1665 (C=O quinone). ¹H-NMR (400 MHz, CDCl₃) δ 2.64 (s, 3H, 3-Me), 2.87 (m, 4H, CH₂CH₂), 3.01 (s, 3H, 1-Me), 3.67 (s, 2H, NH₂), 4.03 (s, 3H, CO₂Me), 6.32 (s, 1H, 6-H), 6.64 (d, *J* = 8.3 Hz, 2H), 6.96 (d, *J* = 8.3 Hz, 2H), 7.18 (dd, *J* = 23.1, 8.4 Hz, 4H), 7.28 (s, 1H, NH). ¹³C-NMR (100 MHz, CDCl₃) δ 181.7, 181.4, 169.2, 161.2, 161.0, 145.6, 144.4, 140.5, 137.8, 134.5, 131.3, 129.9, 129.3, 125.1, 122.9, 119.9, 115.3, 102.1, 53.0, 37.7, 36.9, 26.1, 22.9. HRMS [M + H]⁺: calculated for C₂₇H₂₅N₃O₄: 456.19181; found: 456.1913.

4-acetyl-7-(4-(4-aminophenethyl)phenylamino)-1,3-dimethylisoquinoline-5,8-dione (7). m.p. 224–225 °C; IR (KBr) ν/cm^{-1} : 3339 (NH), 3224, and 3183 (NH₂), 1671 (C=O acetyl) and 1612 (C=O quinone), ¹H-NMR (400 MHz, CDCl₃) δ 2.53 (s, 3H, COMe), 2.56 (s, 3H, 3-Me), 2.85 (m, 4H, CH₂CH₂), 2.98 (s, 3H, 1-Me), 3.60 (s, 2H, NH₂), 6.28 (s, 1H, 6-H), 6.62 (d, *J* = 8.3 Hz, 2H), 6.93 (d, *J* = 8.2 Hz, 2H), 7.16 (dd, *J* = 23.8, 8.4 Hz, 4H), 7.72 (s, 1H, NH). ¹³C-NMR (100 MHz, CDCl₃) δ 22.9, 25.9, 31.1, 36.9, 37.7, 101.7, 115.3, 120.0, 123.0, 129.3, 129.9, 131.2, 133.5, 134.4, 137.9, 140.6, 144.5, 145.9, 159.8, 160.4, 181.7, 182.3, 203.8. HRMS [M + H]⁺: calcd for C₂₇H₂₅N₃O₃: 440.19689; found:440.1966.

Methyl 7-(4-(4-(1,4-dioxo-1,4-dihydronaphthalene-2-ylamino)benzyl)phenylamino)-1,3-dimethyl-5,8-dioxo-5,8-dihydroisoquinoline-4-carboxylate (10). m.p. 186 °C; IR (KBr) ν/cm^{-1} : 3337 (NH), 1720 (C=O ester), 1673 and 1666 (C=O quinone). ¹H-NMR (400 MHz, CDCl₃) δ 2.61 (s, 3H, 3-Me), 2.99 (s, 3H, 1-Me), 4.00 (s, 5H, CO₂Me, CH₂), 6.32 (s, 1H, CH), 6.38 (s, 1H, CH), 7.21 (m, 8H, arom), 7.54 (s, 1H, NH), 7.67 (m, 3H, NH, CH), 7.76 (t, *J* = 8.3 Hz, 1H, CH), 8.11 (t, *J* = 6.7 Hz, 1H, CH). ¹³C-NMR (100 MHz, CDCl₃) δ 181.5, 181.1, 180.4, 177.0, 173.2, 169.3, 161.7, 162.1, 144.8, 141.3, 139.2, 138.8, 137.1, 135.5, 134.8, 133.3, 132.9, 131.3, 130.7, 130.4, 129.0, 127.7, 127.0, 124.1, 123.4, 102.5, 67.5, 53.3, 39.1, 32.7, 22.1. HRMS [M + H]⁺: calculated for C₃₆H₂₇N₃O₆: 598.19729; found: 598.1971.

Methyl 7-(4-(4-(3-chloro-1,4-dioxo-1,4-dihydronaphthalene-2-ylamino)benzyl)phenylamino)-1,3-dimethyl-5,8-dioxo-5,8-dihydroisoquinoline-4-carboxylate (11). m.p. 268–270 °C; IR (KBr) ν/cm^{-1} : 3323 (NH), 1719 (C=O ester), 1681 and 1678 (C=O quinone), 721 (C-Cl). ¹H-NMR (400 MHz, CDCl₃) δ 2.61 (s, 3H, 3-Me), 2.99 (s, 3H, 1-Me), 4.00 (s, 3H, CO₂Me), 4.01 (m, 2H, CH₂), 6.32 (s, 1H, 6-H), 7.03 (d, *J* = 8.3 Hz, 2H), 7.17 (m, 4H, arom), 7.24 (m, 2H, arom), 7.69 (m, 3H, NH, CH), 7.76 (m, 1H, CH), 8.12 (d, *J* = 7.5 Hz, 1H, CH), 8.19 (d, *J* = 7.6 Hz, 1H, CH). ¹³C-NMR (100 MHz, CDCl₃) δ 181.8, 181.5, 180.7, 177.6, 173.7, 169.3, 161.4, 161.1, 145.7, 141.7, 139.3, 138.2, 137.9, 135.9, 135.2, 133.1, 132.8, 131.0, 130.4, 130.0, 129.0, 127.3, 127.2, 124.7, 123.3, 102.4, 66.9, 53.2, 38.9, 32.1, 22.8. HRMS [M + H]⁺: calculated for C₃₆H₂₆ClN₃O₆: 632.15831; found:632.1582.

Methyl 7-(4-(4-(3-chloro-1,4-dioxo-1,4-dihydronaphthalen-2-ylamino)phenethyl)phenylamino)-1,3-dimethyl-5,8-dioxo-5,8-dihydroisoquinoline-4-carboxylate (12). m.p. 263–265 °C; IR (KBr) ν/cm^{-1} : 3307 (NH), 1722 (C=O ester), 1679, and 1675 (C=O quinone), 720 (C-Cl). ¹H-NMR (400 MHz, CDCl₃) δ 2.61 (s, 3H, 3-Me), 2.95 (s, 4H, CH₂CH₂), 2.99 (s, 3H, 1-Me), 4.00 (s, 3H, CO₂Me), 6.29 (s, 1H, 6-H), 7.05 (dd, *J* = 41.2, 8 Hz, 4H, arom), 7.16 (q, *J* = 8.5 Hz, 4H, arom), 7.69 (m, 3H, CH, NH), 7.76 (t, *J* = 7.5 Hz, 1H, CH), 8.11 (d, *J* = 7.6 Hz, 1H, CH), 8.19 (d, *J* = 7.6 Hz, 1H, CH). ¹³C-NMR (100 MHz, CDCl₃) δ 181.6, 181.4, 180.6, 177.5, 169.2, 161.2, 160.9, 145.6, 141.2, 139.7, 138.9, 137.8, 135.5, 135.0, 134.8, 132.9, 132.7, 129.9, 129.8, 128.5, 127.1, 126.9, 125.1, 124.5, 123.0, 119.9, 117.2, 114.4, 102.2, 23.0, 26.1, 29.7, 37.2. HRMS [M + H]⁺: calculated for C₃₇H₂₈ClN₃O₆: 646.17396; found: 646.1796.

Dimethyl-7,7'-(4,4'-methylenebis(4,1-phenylene))bis(azanediy))bis(1,3-dimethyl-5,8-dioxo-5,8-dihydroisoquinoline-4-carboxylate) (13). m.p. 199–200 °C; IR (KBr): ν/cm^{-1} : 3446 (NH), 1736 (C=O ester), 1652 and 1647 (C=O quinone). ¹H-NMR (CDCl₃) δ 2.64 (s, 6H, 3-Me), 3.02 (s, 6H, 1-Me), 4.03 (s, 8H, CH₂ and CO₂Me), 6.34 (s, 1H, 6-H), 7.26 (m, 8H, arom.), 7.73 (s, 2H, NH). ¹³C-NMR (100 MHz, CDCl₃) δ 181.6, 181.4, 169.1, 161.3, 160.9, 145.5, 138.8, 137.8, 135.2, 130.2, 125.1, 123.2, 119.9, 102.3, 53.0, 40.8, 26.1, 22.93. HRMS [M + H]⁺: calculated for C₃₉H₃₂N₄O₈: 685.2293; found: 685.2208.

Dimethyl-7,7'-(4,4'-(ethane-1,2-diyl))bis(4,1-phenylene))bis(azanediy))bis(1,3-dimethyl-5,8-dioxo-5,8-dihydroisoquinoline-4-carboxylate) (14). m.p. 290–293 °C; IR (KBr) ν/cm^{-1} : 3315 (NH), 1730 (C=O ester), 1650 and 1649 (C=O

quinone). $^1\text{H-NMR}$ (400 MHz, CDCl_3) δ 2.53 (s, 6H, 3-Me), 2.56 (s, 6H, 1-Me), 2.96 (s, 4H, CH_2CH_2), 2.99 (s, 6H, CO_2Me), 6.28 (s, 2H, 6-H), 7.18 (q, $J = 8.5$ Hz, 8H, arom), 7.73 (s, 2H, NH). $^{13}\text{C-NMR}$ (100 MHz, CDCl_3) δ 203.8, 182.7, 182.1, 160.8, 160.2, 146.4, 140.0, 138.2, 135.3, 133.9, 130.3, 123.6, 120.4, 102.3, 37.4, 31.3, 26.2, 23.2. HRMS $[\text{M} + \text{H}]^+$: calculated for $\text{C}_{40}\text{H}_{34}\text{N}_4\text{O}_8$: 699.24496; found: 699.2449.

7,7'-(4,4'-(ethane-1,2-diyl)bis(4,1-phenylene))bis(azanediyl)bis(4-acetyl-1,3-dimethylisoquinoline-5,8-dione) (15). m.p. 245–246 °C; IR (KBr) ν/cm^{-1} 3163 (NH), 1693 (C=O acetyl). $^1\text{H-NMR}$ (400 MHz, CDCl_3) δ 2.52 (s, 6H, COMe), 2.56 (s, 6H, 3-Me), 2.96 (s, 4H, CH_2CH_2), 2.99 (s, 6H, 1-Me), 6.27 (s, 2H, 6-H), 7.18 (q, $J = 8.6$ Hz, 8H, arom), 7.74 (s, 2H, NH). $^{13}\text{C-NMR}$ (100 MHz, CDCl_3) δ 203.8, 182.3, 181.6, 160.5, 159.8, 145.9, 139.6, 137.8, 134.6, 133.3, 130.0, 123.2, 101.8, 60.4, 37.1, 31.1, 26.0, 23.0. HRMS $[\text{M} + \text{H}]^+$: calculated for $\text{C}_{40}\text{H}_{34}\text{N}_4\text{O}_6$: 667.25513; found: 667.2570.

3.3. Electrochemical Measurement

The electrochemical measurements were performed in an electrochemical three electrodes cell. Calomel saturated electrode ($\text{SCE}_{\text{sat.}}$) and platinum wire were used as a reference (implementing a Luggin capillary system) and as a counter electrode, respectively. Glassy carbon electrode was used as a working electrode (area: 0.196 cm^2 , Pine Instrument). The measurements were performed using a bipotentiostat (CH Instrument, CH1720E) in acetonitrile containing 0.1 M tetrabutylammonium perchlorate (TBAP) at room temperature. Before the measurements, the solution was deoxygenated using N_2 as purging gas for 15 min.

The half-wave potential ($E_{1/2}$) of the quinone compounds were characterized by cyclic voltammetry in a potential range from -1.9 or -1.5 to 0.5 V at a scan rate of 0.1 V s^{-1} . The $E_{1/2}$ was calculated as the average between the anodic and cathodic peak ($(E_{\text{pa}} + E_{\text{pc}})/2$) [59]. In addition, square wave voltammetry (SWV) was carried out (from -1.5 to -0.5 V vs SCE) to corroborate the half-wave potential, using acetonitrile containing 0.1 M tetrabutylammonium perchlorate (TBAP) at room temperature and purging with N_2 gas for 15 min (Supplementary Figures S1–S8, Cyclic voltammetry and square wave voltammetry (SWV)).

The number of electrons transferred in the faradaic process (E_{pa} or E_{pc}) was determined by coulometric measurements. The tests were performed at a fixed potential 0.1 V higher than the highest anodic peak determined by cyclic voltammetry for two hours. The number of electrons was calculated considering the total charge (Q_{net}) and using the Faraday equation that relates the charge to each mole of quinone studied. ($Q_{\text{net}} = nFz$) [59] where, n = number of moles of the compound, F = Faraday constant (96.487 C mol^{-1}) and z = number of transferred electrons [59]. The concentration of the compounds was 1×10^{-5} M in a total volume of 10 mL.

4. Conclusions

In conclusion, we have synthesized a series of novel heterodimers containing the cytotoxic 7-phenylaminoisoquinolinequinone and 2-phenylaminonaphthoquinone pharmacophores connected through methylene and ethylene spacers. The access to the target heterodimers and their corresponding monomers was performed both through oxidative amination reactions assisted by ultrasound and $\text{CeCl}_3 \cdot 7\text{H}_2\text{O}$ catalysis “in water”. This eco-friendly procedure was successfully extended to the one-pot synthesis of homodimers derived of the 7-phenylaminoisoquinolinequinone pharmacophore. For the mono and dimeric compounds, it was determined that the corresponding first potentials ($E_{1/2}$) are reversible while the second potentials ($E_{1/2}^{\text{II}}$) are quasi reversible ($\Delta E_{1/2}^{\text{II}}$). Furthermore, it was also established that during the oxidation process associated with the potential $E_{1/2}$, the net charge consumption for the monomers is close to 10 mC, while for the heterodimers and homodimers is nearly 20 mC. These facts indicate that in the case of homo- and heterodimers two semiquinone anion radical species are simultaneously generated in the same molecule at similar formal $E_{1/2}$ potentials (via two-electron).

Supplementary Materials: Supplementary materials are available online. The Cyclic voltammetry and square wave voltammetry (SWV) of compounds 5–7 and 10–12, 14, 15 are available as supporting data.

Author Contributions: J.A.I. proposed the subject and designed the study, J.F. and A.D. carried out the chemical experiments, F.J.R. and C.A.Z. performed electrochemical data analysis, and J.A.V. wrote the article.

Funding: The authors thank Vicerrectoría de Investigación, Desarrollo e Innovación, Universidad de Santiago de Chile. DICYT Project No. 021841IR.

Conflicts of Interest: The authors declare no conflict of interest.

Abbreviations

DDM	4,4'-Diaminodiphenylmethane
IR	Infrared
2D-NMR	Bidimensional Nuclear Magnetic Resonance
HRMS	High Resolution Mass Spectroscopy
SCE	Calomel Saturated Electrode
TBAP	Tetrabutylammonium perchlorate
MIC	Minimal Inhibitory Concentration

References

1. Thomson, R.H. *Naturally Occurring Quinones III. Recent Advances*, 3rd ed.; Chapman and Hall: Lincoln, UK, 1987.
2. Sanchez-cruz, P.; Alegria, A.E. Quinone-Enhanced Reduction of Nitric Oxide by Xanthine/Xanthine Oxidase. *Chem. Res. Toxicol.* **2009**, *22*, 818–823. [[CrossRef](#)] [[PubMed](#)]
3. Sagar, S.; Esau, L.; Moosa, B.; Khashab, N.M.; Bajic, V.B.; Kaur, M. Cytotoxicity and Apoptosis Induced by a Plumbagin Derivative in Estrogen Positive MCF-7 Breast Cancer Cells. *Anticancer. Agents Med. Chem.* **2014**, *14*, 170–180. [[CrossRef](#)] [[PubMed](#)]
4. Simic, M.G.; Bergtold, D.S.; Karam, L.R. Generation of oxy radicals in biosystems. *Mutat. Res.* **1989**, *214*, 3–12. [[CrossRef](#)]
5. Bolton, J.L.; Trush, M.A.; Penning, T.M.; Dryhurst, G.; Monks, T.J. Role of Quinones in Toxicology. *Chem. Res. Toxicol.* **2000**, *13*, 135–160. [[CrossRef](#)]
6. Powis, G. Metabolism and reactions of quinoid anticancer agents. *Pharmacol. Ther.* **1987**, *35*, 57–162. [[CrossRef](#)]
7. O'Brien, P.J. Molecular mechanisms of quinone cytotoxicity. *Chem. Biol. Interact.* **1991**, *80*, 1–41. [[CrossRef](#)]
8. Paz, M.M.; Das, A.; Palom, Y.; He, Q.; Tomasz, M. Selective Activation of Mitomycin A by Thiols To Form DNA Cross-links and Monoadducts: Biochemical Basis for the Modulation of Mitomycin Cytotoxicity by the Quinone Redox Potential. *J. Med. Chem.* **2001**, *44*, 2834–2842. [[CrossRef](#)]
9. Tudor, G.; Gutierrez, P.; Aguilera-Gutierrez, A.; Sausville, E.A. Cytotoxicity and apoptosis of benzoquinones: Redox cycling, cytochrome c release, and BAD protein expression. *Biochem. Pharmacol.* **2003**, *65*, 1061–1075. [[CrossRef](#)]
10. Wellington, K.W. Understanding cancer and the anticancer activities of naphthoquinones—A review. *RSC Adv.* **2015**, *26*, 20309–20338. [[CrossRef](#)]
11. Li, K.; Wang, B.; Zheng, L.; Yang, K.; Li, Y.; Hu, M.; He, D. Target ROS to induce apoptosis and cell cycle arrest by 5,7-dimethoxy-1,4-naphthoquinone derivative. *Bioorg. Med. Chem. Lett.* **2018**, *28*, 273–277. [[CrossRef](#)]
12. Jiang, X.; Meng, L.; Wang, Y.; Zhang, Y. Novel 1,4-Naphthoquinone derivatives induce apoptosis via ROS-mediated p38/MAPK, Akt and STAT3 signaling in human hepatoma Hep3B cells. *Int. J. Biochem. Cell. Biol.* **2018**, *96*, 9–19. [[CrossRef](#)]
13. Monks, T.; Jones, D. The Metabolism and Toxicity of Quinones, Quinonimines, Quinone Methides, and Quinone-Thioethers. *Curr. Drug. Metab.* **2002**, *3*, 425–438. [[CrossRef](#)] [[PubMed](#)]
14. Monks, T.J.; Hanzlik, R.P.; Cohen, G.M.; Ross, D.; Graham, D.G. Quinone chemistry and toxicity. *Toxicol. Appl. Pharmacol.* **1992**, *112*, 2–16. [[CrossRef](#)]
15. Kim, H.J.; Mun, J.Y.; Chun, Y.J.; Choi, K.H.; Ham, S.W.; Kim, M.Y. Effects of a naphthoquinone analog on tumor growth and apoptosis induction. *Arch. Pharm. Res.* **2003**, *26*, 405–410. [[CrossRef](#)]
16. Kondracki, M.-L.; Guyot, M. Smenospongine: A cytotoxic and antimicrobial aminoquinone isolated from sp. *Tetrahedron Lett.* **1987**, *28*, 5815–5818. [[CrossRef](#)]

17. Kong, D.; Yamori, T.; Kobayashi, M.; Duan, H. Antiproliferative and Antiangiogenic Activities of Smenospongine, a Marine Sponge Sesquiterpene Aminoquinone Dixin. *Mar. Drugs* **2011**, *9*, 154–161. [[CrossRef](#)] [[PubMed](#)]
18. Bolzán, A.D.; Bianchi, M.S. Genotoxicity of streptonigrin: A review. *Mutat. Res.* **2001**, *488*, 25–37. [[CrossRef](#)]
19. Dale, L.; Yasuda, M.; Steven, D. Streptonigrin and Lavendamycin Partial Structures. Probes for the Minimum, Potent Pharmacophore of Streptonigrin, Lavendamycin, and Synthetic Quinoline-5,8-diones. *J. Med. Chem.* **1987**, *30*, 1918–1928. [[CrossRef](#)]
20. Rao, K.V.; Cullen, W.P. Streptonigrin, an antitumor substance. I. Isolation and characterization. In *Antibiotics Annual 1959–1960*; Welch, H., Martí-Ibáñez, F., Eds.; Medical Encyclopedia, Inc.: New York, NY, USA, 1960.
21. Rao, K.V.; Biemann, K.; Woodward, R.B. The structure of streptonigrin. *J. Am. Chem. Soc.* **1963**, *85*, 2532–2533. [[CrossRef](#)]
22. Harding, M.M.; Long, G.V.; Brown, C.L. Solution Conformation of the Antitumor Drug Streptonigrin. *J. Med. Chem.* **1993**, *36*, 3056–3060. [[CrossRef](#)]
23. Hawas, U.W.; Shaaban, M.; Shaaban, K.A.; Speitling, M.; Maier, A.; Kelter, G.; Fiebig, H.H.; Meiners, M.; Helmke, E.; Laatsch, H. Mansouramycins A–D, Cytotoxic Isoquinolinequinones from a Marine Streptomyces. *J. Nat. Prod.* **2009**, *72*, 2120–2124. [[CrossRef](#)] [[PubMed](#)]
24. Kuang, S.; Liu, G.; Cao, R.; Zhang, L.; Yu, Q.; Sun, C. Mansouramycin C kills cancer cells through reactive oxygen species production mediated by opening of mitochondrial permeability transition pore. *Oncotarget* **2017**, *8*, 104057–104071. [[CrossRef](#)] [[PubMed](#)]
25. Benites, J.; Valderrama, J.A.; Ramos, M.; Valenzuela, M.; Guerrero-castilla, A.; Muccioli, G.G.; Calderon, P.B. Half-Wave Potentials and In Vitro Cytotoxic Evaluation of 3-Acylated 2,5-Bis(phenylamino)-1,4-benzoquinones on Cancer Cells. *Molecules* **2019**, *24*, 1780. [[CrossRef](#)] [[PubMed](#)]
26. Benites, J.; Valderrama, J.A.; Bettiga, K.; Curi, R.; Buc, P.; Verrax, J. Biological evaluation of donor-acceptor aminonaphthoquinones as antitumor agents. *Eur. J. Med. Chem.* **2010**, *45*, 6052–6057. [[CrossRef](#)] [[PubMed](#)]
27. Tandon, V.K.; Chhor, R.B.; Singh, R.V.; Yadav, D.B. Design, synthesis and evaluation of novel 1,4-naphthoquinone derivatives as antifungal and anticancer agents. *Bioorg. Med. Chem. Lett.* **2004**, *14*, 1079–1083. [[CrossRef](#)]
28. Francisco, A.I.; Casellato, A.; Neves, A.P.; Carneiro, J.W.d.M.; Vargas, M.D.; Visentin, L.do.C.; Magalhães, A.; Câmara, C.A.; Pessoa, C.; Costa-Lotufo, L.V.; et al. Novel 2-(R-phenyl)amino-3-(2-methylpropenyl)-[1,4]-naphthoquinones: Synthesis, characterization, electrochemical behavior and antitumor activity. *J. Braz. Chem. Soc.* **2010**, *21*, 169–178. [[CrossRef](#)]
29. Ibacache, J.A.; Delgado, V.; Benites, J.; Theoduloz, C.; Arancibia, V.; Muccioli, G.G.; Valderrama, J.A. Synthesis, Half-Wave Potentials and Antiproliferative Activity of 1-Aryl-substituted Aminoisoquinolinequinones. *Molecules* **2014**, *19*, 726–739. [[CrossRef](#)]
30. Pathania, D.; Kuang, Y.; Sechi, M.; Neamati, N. Mechanisms underlying the cytotoxicity of a novel quinazolinedione-based redox modulator, QD232, in pancreatic cancer cells. *Br. J. Pharmacol.* **2014**, *172*, 50–63. [[CrossRef](#)]
31. Benites, J.; Valderrama, J.A.; Ramos, M.; Muccioli, G.G. Targeting Akt as strategy to kill cancer cells using 3-substituted 5-anilinobenzo[c]isoxazolequinones: A preliminary study. *Biomed. Pharmacother.* **2018**, *97*, 778–783. [[CrossRef](#)]
32. Ryu, C.; Kang, H.; Lee, K.; Nam, A. 5-Arylamino-2-methyl-4,7-dioxobenzothiazoles as Inhibitors of Cyclin-Dependent Kinase 4 and Cytotoxic Agents. *Bioorg. Med. Chem. Lett.* **2000**, *10*, 461–464. [[CrossRef](#)]
33. Kongkathip, N.; Kongkathip, B.; Siripong, P.; Sangma, C.; Luangkamin, S.; Niyomdech, M.; Pattanapa, S.; Piyaviriyagul, S.; Kongsaree, P. Potent antitumor activity of synthetic 1,2-naphthoquinones and 1,4-naphthoquinones. *Bioorganic. Med. Chem.* **2003**, *11*, 3179–3191. [[CrossRef](#)]
34. Bonifazi, E.L.; Rios-Luci, C.; León, L.G.; Burton, G.; Padrón, J.M.; Misico, R.I. Antiproliferative activity of synthetic naphthoquinones related to lapachol. First synthesis of 5-hydroxylapachol. *Bioorganic Med. Chem.* **2010**, *18*, 2621–2630. [[CrossRef](#)] [[PubMed](#)]
35. Duchowicz, P.R.; Bennardi, D.O.; Baceo, D.E.; Bonifazi, E.L.; Rios-Luci, C.; Padrón, J.M.; Burton, G.; Misico, R.I. QSAR on antiproliferative naphthoquinones based on a conformation-independent approach. *Eur. J. Med. Chem.* **2014**, *77*, 176–184. [[CrossRef](#)] [[PubMed](#)]

36. Baiju, T.V.; Almeida, R.G.; Sivanandan, S.T.; de Simone, C.A.; Brito, L.M.; Cavalcanti, B.C.; Pessoa, C.; Namboothiri, I.N.N.; da Silva Júnior, E.N. Quinonoid compounds via reactions of lawsone and 2-aminonaphthoquinone with α - bromonitroalkenes and nitroallylic acetates: Structural diversity by C-ring modification and cytotoxic evaluation against cancer cells. *Eur. J. Med. Chem.* **2018**, *151*, 686–704. [[CrossRef](#)] [[PubMed](#)]
37. Valderrama, J.A.; Cabrera, M.; Benites, J.; Ríos, D.; Inostroza-Rivera, R.; Muccioli, G.G.; Calderon, P.B. Synthetic approaches and: In vitro cytotoxic evaluation of 2-acyl-3-(3,4,5-trimethoxyanilino)-1,4-naphthoquinones. *RSC. Adv.* **2017**, *7*, 24813–24821. [[CrossRef](#)]
38. Valderrama, J.A.; Andrea, I.J.; Arancibia, V.; Rodriguez, J.; Theoduloz, C. Studies on quinones. Part 45: Novel 7-aminoisoquinoline-5,8-quinone derivatives with antitumor properties on cancer cell lines. *Bioorganic Med. Chem.* **2009**, *17*, 2894–2901. [[CrossRef](#)]
39. Delgado, V.; Ibacache, A.; Theoduloz, C.; Valderrama, J.A. Synthesis and in vitro cytotoxic evaluation of aminoquinones structurally related to marine isoquinolinequinones. *Molecules* **2012**, *17*, 7042–7056. [[CrossRef](#)]
40. Aguilar-Martinez, M.; Cuevas, G.; Jimenez-Estrada, M.; Gonzalez, I.; Lotina- Henssen, B.; Macias-Ruvalcaba, N. An experimental and theoretical study of the substituent effects on the redox properties of 2-[(R-phenyl)-amine]-1,4-naphthalenediones in acetonitrile. *J. Org. Chem.* **1999**, *64*, 3684–3694. [[CrossRef](#)]
41. Bolognesi, M.L.; Banzi, R.; Bartolini, M.; Cavalli, A.; Tarozzi, A.; Andrisano, V.; Minarini, A.; Rosini, M.; Tumiatti, V.; Bergamini, C.; et al. Novel class of quinone-bearing polyamines as multi-target-directed ligands to combat Alzheimer's disease. *J. Med. Chem.* **2007**, *50*, 4882–4897. [[CrossRef](#)]
42. Bernardo, P.H.; Khanijou, J.K.; Lam, T.H.; Tong, J.C.; Chai, C.L.L. Synthesis and potent cytotoxic activity of 8- and 9-anilinophenanthridine- 7,10-diones. *Tetrahedron Lett.* **2011**, *52*, 92–94. [[CrossRef](#)]
43. Sanna, V.; Nurra, S.; Pala, N.; Marceddu, S.; Pathania, D.; Neamati, N.; Sechi, M. Targeted Nanoparticles for the Delivery of Novel Bioactive Molecules to Pancreatic Cancer Cells. *J. Med. Chem.* **2016**, *59*, 5209–5220. [[CrossRef](#)] [[PubMed](#)]
44. Lisboa, C.D.S.; Santos, V.G.; Vaz, B.G.; De Lucas, N.C.; Eberlin, M.N.; Garden, S.J. C-H functionalization of 1,4-naphthoquinone by oxidative coupling with anilines in the presence of a catalytic quantity of copper(II) acetate. *J. Org. Chem.* **2011**, *76*, 5264–5273. [[CrossRef](#)] [[PubMed](#)]
45. Beck, R.; Verrax, J.; Gonze, T.; Zappone, M.; Curi, R.; Taper, H.; Feron, O.; Buc, P. Hsp90 cleavage by an oxidative stress leads to its client proteins degradation and cancer cell death. *Biochem. Pharmacol. Ogy.* **2009**, *77*, 375–383. [[CrossRef](#)] [[PubMed](#)]
46. Pathania, D.; Sechi, M.; Palomba, M.; Sanna, V.; Berrettini, F.; Sias, A.; Taheri, L.; Neamati, N. Design and discovery of novel quinazolinedione-based redox modulators as therapies for pancreatic cancer. *Biochim. Biophys. Acta* **2014**, *1840*, 332–343. [[CrossRef](#)] [[PubMed](#)]
47. Ravichandiran, P.; Sheet, S.; Premnath, D.; Kim, A.R. 1,4-Naphthoquinone Analogues: Potent Antibacterial Agents and Mode of Action Evaluation. *Molecules* **2019**, *24*, 1437. [[CrossRef](#)]
48. Ferraz, P.A.; de Abreu, F.C.; Pinto, A.V.; Glezer, V.; Tonholo, J.; Goulart, M.O. Electrochemical aspects of the reduction of biologically active 2-hydroxy-3-alkyl-1,4-naphthoquinones. *J. Electroanal. Chem.* **2001**, *507*, 275–286. [[CrossRef](#)]
49. González, F.J.; Aceves, J.M.; Miranda, R.; González, I. The electrochemical reduction of perezone in the presence of benzoic acid in acetonitrile. *J. Electroanal. Chem. Interfacial. Electrochem.* **1991**, *310*, 293–303. [[CrossRef](#)]
50. Hillard, E.A.; De Abreu, F.C.; Ferreira, D.C.M.; Jaouen, G.; Goulart, M.O.F.; Amatore, C. Electrochemical parameters and techniques in drug development, with an emphasis on quinones and related compounds. *Chem. Commun.* **2008**, 2612–2628. [[CrossRef](#)]
51. Armendáriz-Vidales, G.; Hernández-Muñoz, L.S.; González, F.J.; De Souza, A.A.; De Abreu, F.C.; Jardim, G.A.M.; Da Silva, E.N.; Goulart, M.O.F.; Frontana, C. Nature of electrogenerated intermediates in nitro-substituted nor- β -lapachones: The structure of radical species during successive electron transfer in multiredox centers. *J. Org. Chem.* **2014**, *79*, 5201–5208. [[CrossRef](#)]

52. Hernández, D.M.; De Moura, M.A.B.F.; Valencia, D.P.; González, F.J.; González, I.; De Abreu, F.C.; Da Silva Júnior, E.N.; Ferreira, V.F.; Pinto, A.V.; Goulart, M.O.F.; et al. Inner reorganization during the radical-biradical transition in a nor- β -lapachone derivative possessing two redox centers. *Org. Biomol. Chem.* **2008**, *6*, 3414–3420. [[CrossRef](#)]
53. Koyama, J.; Morita, I.; Kobayashi, N.; Osakai, T. Correlation of redox potentials and inhibitory effects on Epstein–Barr virus activation of naphthoquinones. *Cancer Lett.* **2003**, *201*, 25–30. [[CrossRef](#)]
54. Ibacache, J.A.; Faundes, J.; Montoya, M.; Meji, S.; Jaime, A. Preparation of Novel Homodimers Derived from Cytotoxic Isoquinolinequinones. A Twin Drug Approach. *Molecules* **2018**, *23*, 439. [[CrossRef](#)] [[PubMed](#)]
55. Delgado, V.; Ibacache, A.; Arancibia, V.; Theoduloz, C.; Valderrama, J.A. Synthesis and in Vitro Antiproliferative Activity of New Phenylaminoisoquinolinequinones against Cancer Cell Lines. *Molecules* **2013**, *18*, 721–734. [[CrossRef](#)] [[PubMed](#)]
56. Puri, S.; Kaur, B.; Parmar, A.; Kumar, H. Applications of Ultrasound in Organic Synthesis - A Green Approach. *Curr. Org. Chem.* **2013**, *17*, 1790–1828. [[CrossRef](#)]
57. Guin, P.S.; Das, S.; Mandal, P.C. Electrochemical Reduction of Quinones in Different Media: A Review. *Int. J. Electrochem.* **2011**, *2011*, 1–22. [[CrossRef](#)]
58. He, P.; Crooks, R.M.; Faulkner, L.R. Adsorption and electrode reactions of disulfonated anthraquinones at mercury electrodes. *J. Phys. Chem.* **2005**, *94*, 1135–1141. [[CrossRef](#)]
59. Bard, A.J.; Faulkner, L.R.; Swain, E.; Robey, C. *Electrochemical Method—Fundamentals and Applications*, 2nd ed.; Harris, D., Swain, E., Robey, C., Aiello, E., Eds.; John Wiley & Sons: New York, NY, USA, 2001; ISBN 0471043729.
60. Patai, S.; Rappoport, Z. (Eds.) *The Chemistry of the Quinonoid Compounds*; John Wiley & Sons: New York, NY, USA, 1988; Chapter 12; Volume 2, ISBN 9780470772119.
61. Skancke, A.; Skancke, P.N. *General and Theoretical Aspects of Quinones*; Patai, S., Rappoport, Z., Eds.; John Wiley & Sons: New York, NY, USA, 1988; Chapter 14; Volume 1, ISBN 9780470772119.
62. Wu, D.; Huang, Y.; Hu, X. A sulfurization-based oligomeric sodium salt as a high-performance organic anode for sodium ion batteries. *Chem. Commun.* **2016**, *52*, 11207–11210. [[CrossRef](#)]
63. Han, C.; Li, H.; Shi, R.; Zhang, T.; Tong, J.; Li, J.; Li, B. Organic quinones towards advanced electrochemical energy storage: Recent advances and challenges. *J. Mater. Chem. A* **2019**, 1–38. [[CrossRef](#)]
64. Mirkhalaf, F.; Tammeveski, K.; Schiffrin, D.J. Substituent effects on the electrocatalytic reduction of oxygen on quinone-modified glassy carbon electrodes. *Phys. Chem. Chem. Phys.* **2004**, *6*, 1321–1327. [[CrossRef](#)]
65. Jardim, G.A.M.; Reis, W.J.; Ribeiro, M.F.; Ottoni, F.M.; Alves, R.J.; Silva, T.L.; Goulart, M.O.F.; Braga, A.L.; Menna-Barreto, R.F.S.; Salomão, K.; et al. On the investigation of hybrid quinones: Synthesis, electrochemical studies and evaluation of trypanocidal activity. *RSC Adv.* **2015**, *5*, 78047–78060. [[CrossRef](#)]
66. Elhabiri, M.; Sidorov, P.; Cesar-Rodo, E.; Marcou, G.; Lanfranchi, D.A.; Davioud-Charvet, E.; Horvath, D.; Varnek, A. Electrochemical properties of substituted 2-methyl-1,4-naphthoquinones: Redox behavior predictions. *Chem.-A Eur. J.* **2015**, *21*, 3415–3424. [[CrossRef](#)] [[PubMed](#)]
67. Turek, A.K.; Hardee, D.J.; Ullman, A.M.; Nocera, D.G.; Jacobsen, E.N. Activation of Electron-Deficient Quinones through Hydrogen-Bond-Donor-Coupled Electron Transfer. *Angew. Chemie.-Int. Ed.* **2016**, *55*, 539–544. [[CrossRef](#)] [[PubMed](#)]

Sample Availability: Samples of the synthesized compounds **5**, **6**, **13** and **15** are available from the corresponding authors.



© 2019 by the authors. Licensee MDPI, Basel, Switzerland. This article is an open access article distributed under the terms and conditions of the Creative Commons Attribution (CC BY) license (<http://creativecommons.org/licenses/by/4.0/>).